NASA TECHNICAL NOTE

NASA TN D-7070

NASA TN D-7070

EXPERIMENTAL PERFORMANCE OF AN INTERNAL RESISTANCE HEATER FOR LANGLEY 6-INCH EXPANSION TUBE DRIVER

by Theodore R. Creel, Jr.

Langley Research Center
Hampton, Va. 23365

NATIONAL AERONAUTICS AND SPACE ADMINISTRATION • WASHINGTON, D. C. • DECEMBER 1972

1. Report No.	2. Government Accession No.	3. Recipient's Catalog No.
NASA TN D-7070		

4. Title and Subtitle	5. Report Date
EXPERIMENTAL PERFORMANCE OF AN INTERNAL RESISTANCE HEATER FOR LANGLEY 6-INCH EXPANSION TUBE DRIVER	December 1972
	6. Performing Organization Code
7. Author(s)	8. Performing Organization Report No.
Theodore R. Creel, Jr.	L-8556
	10. Work Unit No.
9. Performing Organization Name and Address	502-07-01-02
NASA Langley Research Center Hampton, Va. 23365	11. Contract or Grant No.
	13. Type of Report and Period Covered
12. Sponsoring Agency Name and Address	Technical Note
National Aeronautics and Space Administration Washington, D.C. 20546	14. Sponsoring Agency Code

15. Supplementary Notes

16. Abstract

An experimental investigation of the heating characteristics of an internal resistance heating element was conducted in the driver of the Langley 6-inch expansion tube to obtain actual operating conditions, to compare these results to theory, and to determine whether any modification need be made to the heater element. The heater was operated in pressurized helium from 1.38 MN/m^2 to 62.1 MN/m^2. This investigation revealed large temperature variations within the heater element caused primarily by area reductions at insulator locations. These large temperature variations were reduced by welding small tabs over all grooves. This experience has shown that a constant area heater element is very important to uniform heating. Previous predictions of heater element and driver gas temperature were unacceptable so new equations were derived. These equations predict element and gas temperature within 10 percent of the test data when either the constant power cycle or the interrupted power cycle is used. The interrupted power cycle is shown to produce a higher average element temperature and, therefore, a higher average driver gas temperature. Visual observation of the heater element, when exposed to the atmosphere with power on, resulted in a decision to limit the heater element to 815 K. Experimental shock Mach numbers are in good agreement with theory.

17. Key Words (Suggested by Author(s))	18. Distribution Statement
Facility Heat transfer Shock tubes Expansion tubes	Unclassified – Unlimited

19. Security Classif. (of this report)	20. Security Classif. (of this page)	21. No. of Pages	22. Price*
Unclassified	Unclassified	25	$3.00

*For sale by the National Technical Information Service, Springfield, Virginia 22151

EXPERIMENTAL PERFORMANCE OF AN INTERNAL RESISTANCE HEATER FOR LANGLEY 6-INCH EXPANSION TUBE DRIVER

By Theodore R. Creel, Jr.
Langley Research Center

SUMMARY

An experimental investigation of the heating characteristics of an internal resistance heating element was conducted in the driver of the Langley 6-inch expansion tube to obtain actual operating conditions, to compare these results to theory, and to determine whether any modification need be made to the heater element. The heater was operated in pressurized helium from 1.38 MN/m^2 to 62.1 MN/m^2. This investigation revealed large temperature variations within the heater element caused primarily by area reductions at insulator locations. These large temperature variations were reduced by welding small tabs over all grooves. This experience has shown that a constant area heater element is very important to uniform heating. Previous predictions of heater element and driver gas temperature were unacceptable, so new equations were derived. These equations predict element and gas temperature within 10 percent of test data when either the constant power cycle or the interrupted power cycle is used. The interrupted power cycle is shown to produce a higher average element temperature and, therefore, a higher average driver gas temperature. Visual observation of the heater element, when exposed to the atmosphere with power on, resulted in a decision to limit the heater element to 815 K. Experimental shock Mach numbers are in good agreement with theory.

INTRODUCTION

Theoretical investigations of the ability of ground facilities to simulate flight conditions of reentering space vehicles (for example, ref. 1) have shown that extremely high velocity and altitude simulation are needed. This simulation can be accomplished by an expansion-tube-type facility. Because of these studies, a pilot model expansion tube was built, and the feasibility of using this technique was reported in reference 2. Additional investigations (refs. 3 and 4) explored further the capabilities of this device and also determined that by adding a nozzle the performance of this facility could be broadened (for example, longer test time).

With this information available, the Langley 6-inch expansion tube was proposed. By using extremely high reservoir pressures and temperatures this facility could simulate the enthalpy-pressure range desired. High-velocity performance in a shock tube or expansion tube requires a driver gas with a high acoustic speed and can be obtained by any of several methods, such as electrical heating by convection, ohmic heating by electrical discharge, multiple diaphragms, combustion, external heat exchangers, magnetic induction techniques, and by using a light gas combined with these heating techniques.

References 5 and 6 studied the feasibility of using these techniques and concluded that the operational characteristics of electrical resistance heating were superior to those of other methods. Of course, each method has some undesirable characteristics which the experimenter must consider. Two of these heating methods, arc discharge and internal resistance heating, have been incorporated into the Langley 6-inch expansion tube to provide flexibility in the operating range. The resistance heater described was designed to heat hydrogen to 555 K at 4.788 MN/m^2. To obtain even greater flexibility of operation, three different size internal resistance heater elements are used. The physical overall dimensions of the corresponding driver chambers are: a 0.152-meter-diameter, 2.438-meter-long chamber; a 0.152-meter-diameter, 4.877-meter-long chamber; and a 0.305-meter-diameter, 2.438-meter-long chamber.

The reason for heating the driver gas is shown by the curves presented in figure 1. These curves show that by heating the driver gas, the shock Mach number obtainable for the same pressure ratio is considerably increased. Alternately, when the shock Mach number is held constant, the pressure ratio needed to obtain this Mach number may be reduced by approximately a factor of 10, provided the driver gas is heated to twice the driven gas temperature. Because the Langley 6-inch expansion tube is designed to use both hydrogen and helium for a driver gas, the two performance curves are presented for comparison.

This paper is a summary of the operating experience gained while using the 0.152-meter-diameter, 2.438-meter-long driver chamber with its corresponding heater element. As all heater elements are essentially the same shape, the experience gained with this element will be applicable to the other elements. During all pressurized phases of the tests, helium was used as the driver gas.

SYMBOLS

A area, m^2

c specific heat of element, J/kg-K

c_v	specific heat of gas at constant volume, J/kg-K
E,R,Q	proportionality constants
h	heat-transfer coefficient, W/m^2-K
K	constant of integration
M	Mach number
m	weight of gas, kg
P	power, kW
T	temperature, K
t	time, sec
W	weight of heater element, kg

Subscripts:

G	driver gas
H	heater element
w	chamber-wall condition
1	initial state in intermediate chamber
4	initial state in driver

Superscript:

*	reference condition

INSTRUMENTATION

The instrumentation of the expansion tube for these tests is typical of shock-tube or expansion-tube operation and is similar to the instrumentation as discussed in reference 2. Where applicable, reference 2 is cited.

Shock speed was measured by two methods. One method was to record the pressure rise at several stations along the tube. The second was to measure the shock speed by microwave as described in reference 2.

Driver chamber and double diaphragm chamber pressures were measured by strain-gage transducers of 0- to 68.94-MN/m^2 pressure. Intermediate-chamber pressures were measured by 0- to 6.9-kN/m^2 quartz piezoelectric gages.

Chromel-alumel thermocouples were used to measure the element temperatures. These thermocouples were attached directly to the element. Experimental gas temperature was measured by a bare-wire chromel-alumel thermocouple located above the element halfway between the element center line and the chamber wall. Pressures and thermocouple data were recorded on a light-beam-type oscillograph having a variety of chart speeds.

APPARATUS

Figure 2 is a schematic of the heating system used in the Langley hot gas radiation research facility expansion tube driver section showing the heating element, automatic controller, and the power supply.

The power supply consists of two silicone controlled rectifier modules to supply an adjustable direct-current output which is obtained by converting 6600-volt 60-hertz, three-phase alternating current to 90- or 180-volt direct current. The equipment may be used in any of the following modes of operation:

(a) Single unit – 10- to 90-volt direct current, 1000- to 20 000-ampere direct current. Duty cycle – 15 minutes on, 120 minutes off.

(b) Two units in parallel – 10- to 90-volt direct current, 2000- to 40 000-ampere direct current. Duty cycle – 5 minutes on, 120 minutes off.

(c) Two units in series – 20- to 180-volt direct current, 1000- to 20 000-ampere direct current. Duty cycle – 5 minutes on, 120 minutes off.

Any of the three modes may be programed by an automatic controller or operated manually. Response time of 0.1 second can be achieved by the system.

The resistance heater control system is a feedback network which automatically controls the power level of the conversion unit output to a resistive heater element. The network senses the current and voltage signal which is used to modulate the electrical energy of the load. Associated with the main control loop are auxiliary circuits for limiting pressure and temperature in the test chamber to preset values. The unit has an automatic diaphragm release circuit which triggers the firing network at a preset chamber pressure. The controller has adjustable controls for gain, reset, and rate and utilizes solid-state operational amplifiers.

The heating element (figs. 3 and 4) is constructed of two parallel modified Y-shaped stainless-steel (type 321) extrusions connected at one end to the power supply by water-cooled beryllium-copper rods (alloy 10), which also mechanically restrain the element, and at the other end by two stainless-steel crossover plates. The two members of the element are separated from each other by H-shaped aluminum oxide insulators. The element is positioned in the driver and insulated from the driver wall by aluminum oxide cylinders (fig. 4), 1.905-cm diameter and 3.175 cm long, spaced at 24.156-cm intervals. These cylindrical insulators are restrained by the channel in the heater element and are securely held in position by a contoured metal retainer at each end of the insulator. The insulator retainers are held in position by socket head cap screws. Additional retaining strength was estimated to be necessary for each downstream retainer, so a shear lip (fig. 4) was machined on the retainer which fits into a groove cut in the channel.

RESULTS AND DISCUSSION

An experimental investigation of the heating characteristics of an internal resistance heating element was conducted in the Langley 6-inch expansion tube of the Langley hot gas radiation research facility to obtain actual operating conditions at atmospheric pressure and in pressurized helium from 1.38 MN/m^2 to 62.1 MN/m^2 and to compare these results to theory. Performance checks of the heater element began with the driver open to the atmosphere so as to permit a number of thermocouples to be attached to the element. During the atmospheric tests of the heater element, several large temperature variations were observed and are illustrated in figure 5. Figure 5(a) is representative of the variation of temperature on the top surface of the heater element, starting with the maximum on the outside near the cylindrical insulator and decreasing as the element center is approached. Each side of the element experienced the temperature variation illustrated in figure 5(b) where the maximum temperature is registered on the extreme portion of the element on the section that holds the cylindrical insulators. The thermocouple located on the bottom outside flange measured a temperature of about 50 K lower than the top flange. In general, the recorded temperatures, as represented by figure 5(c),

along the length of the heater element were higher in the middle of the element than at either end, possibly because of the larger connecting cross sections at the ends and the water cooling of the copper rods.

During the development of the heater, the most persistent problem was the attainment of a uniform heater temperature. Local temperature variations detected by thermocouples revealed hot spots approximately 200 K greater than any other measured temperature. These local hot spots, which occurred at the grooves cut in the Y-shaped heater element for the lip on the cylindrical insulator retainer (fig. 4), mentioned previously in the description, resulted in heater element color changes shown as dark areas separated by large areas in figure 6. Section A-A of figure 4 shows the extent of cross-sectional area reduction caused by a machined groove for the downstream insulator retainer lip. This machined groove resulted in 22-percent cross-sectional area reduction which the insulator retainer lip, although closely fitted into the groove, apparently did not replace. These area reductions became regions of high current density; that is, local hot spots. As a confirmation of the thermocouples, power was applied until a red glow was observed at the point of reduced cross-sectional area. From table 8 chapter 4, page 6 of reference 7, this temperature was estimated to be 1050 K. Small tabs of similar material were welded over the grooves to replace the lost cross-sectional area. Thermocouples and visual observations indicated that the previous hot spots became cold spots with the new hot spots covering a much larger area. However, the differences were not so extreme and the element was now at an average temperature closer to the maximum temperature of any point of the heater element.

Another problem discovered during the atmospheric tests is the relatively low temperature of the downstream crossover plates (which were shallow U-shaped plates, horizontally positioned on the top and bottom of the element connecting the opposite pieces of the element near the diaphragm (fig. 7)) when compared to the main section of the heater element. The plate cross-sectional area was reduced by half; but because of structural limitations, further reductions were not considered. Also, the upstream half of the crossover plate was apparently heated much more than the downstream half, thereby creating a sharp temperature gradient in the plate.

During these atmospheric tests, the heater element was subjected to extreme thermal stress, resulting in warping of the element, but because it is supported by the cylindrical insulator and the driver chamber wall, it could still be removed from the driver for inspection and maintenance. Failure of these cylindrical insulators has occurred but rarely. Unfortunately, relative movement between the heater element sides caused at least one H-shaped insulator (fig. 7) to break during a run. Based upon the results of the atmospheric tests, a decision was made to lower the operating temperature of the heater from 923 K to 815 K.

The atmospheric tests of the internal resistance heater were followed by tests to determine the operating characteristics of the heater, as measured by the pressure-temperature rise of the driver gas when pressurized. For this phase of the tests, a diaphragm was fitted with glands so that seven thermocouples could be used in the driver over a pressure range of 0 to 6.9 MN/m^2. Two of these thermocouples were used to measure the element temperature at suspected hot spots with three thermocouples bracketing these hot spots. One thermocouple used to measure gas temperature was located half the distance between the element center line and the top of the driver chamber. The remaining thermocouple measured driver chamber wall temperature.

Various temperatures obtained during one 19-second application of power to the heater element when immersed in pressurized helium are presented in figure 8. Although element temperatures were measured at five locations, only the maximum and average temperature is presented in figure 8. As can be seen, the experimental maximum element temperature is approximately 100 K higher than the theoretical temperature (assumed uniform) predicted by reference 8. This discrepancy is caused by the nonuniform element area producing high current densities, whereas the theory of reference 8 assumes uniform area along the length of the heater element. Also shown is the average of the five element temperatures to illustrate the effect of area reduction on local temperature. This average temperature is approximately 150 K less than the temperature predicted by reference 8 by the end of the test.

The experimental gas temperature (fig. 8) was measured by a bare-wire chromel-alumel thermocouple which was exposed to radiation from the heater element. Resultant radiant heating could have been one reason for the experimental gas temperature being higher than the gas temperature calculated from the pressure rise. Calculated gas temperature was obtained from the ideal gas relation by assuming constant volume and gas mass. Another reason for the discrepancy between the experimental and calculated gas temperatures could be that natural convection in the chamber would tend to circulate the hotter gas to the top of the driver chamber. Both the measured and calculated gas temperatures are well below the theoretical gas temperature predicted by reference 8. This discrepancy probably means that the heat-transfer coefficients (heater to gas) used in the theory of reference 8 are greater than actual.

Although the heater element reached a high temperature, the duration of the power-on phase was such that the uninsulated driver chamber wall temperature did not appreciably increase. The trends shown in figure 8 are characteristic of all tests.

After completion of a series of no-flow tests (fig. 8 is typical), all but three thermocouples leading into the driver chamber were removed. Two of the remaining thermocouples measured the element temperature at different locations, thus insuring a

thermocouple reading in case one failed. The third thermocouple was to be used to measure driver gas temperature, but after several failures of this thermocouple, pressure rise was used for gas temperature indication.

The driver gas heating calculations used in the design of the present heater, which were taken from reference 8, showed rather poor agreement with the experimental results (see fig. 8). An improved relation was needed that would correlate closely with the experimentally observed heating rates both for use as operational guidelines and to evaluate the performance of the heater.

By starting with a fundamental heat balance and neglecting radiation effects, the heat transferred to the gas minus the heat transferred to the wall yields the net increase in driver gas energy; thus the equation can be written as

$$h_H A_H(T_H - T_G) - h_w A_w(T_G - T_w) = m_G c_{v_G} \frac{dT_G}{dt} \tag{1}$$

It is assumed here that the temperatures of the heater, gas, and wall can each be characterized by a single value at any instant of time. Incremental values used are $T_H = T_G = T_w$ at $t = 0$. Define

$$B = h_H A_H$$

$$C = h_w A_w$$

$$D = m_G c_{v_G}$$

then equation (1) becomes

$$B(T_H - T_G) - C(T_G - T_w) = D\frac{dT_G}{dt} \tag{2}$$

or

$$T_G + \frac{D}{B + C}\frac{dT_G}{dt} = \frac{B}{B + C}T_H + \frac{C}{B + C}T_w \tag{3}$$

For the conditions of this experiment, the second term on the left-hand side of equation (3) was found to be small by comparison with the others and as a first approximation may be neglected. Thus

$$T_G = \frac{B}{B + C}T_H + \frac{C}{B + C}T_w \tag{4}$$

An examination of the wall temperature measurements indicated an approximately linear increase with time

$$T_w = Et$$

so that

$$T_G = \frac{B}{B + C}T_H + \frac{CE}{B + C}t \tag{5}$$

Curve fitting equation (5) to experimental results of the present investigation yielded

$$T_G = 0.3T_H + 0.55t \tag{6}$$

An equation for predicting heater element temperature was also obtained from simple heat balance considerations with the aid of the simplifying assumptions that h_H, C, and power are constant with time. The heat-flow balance for the heater element was considered to be

$$P = A_H h_H (T_H - T_G) + W_H c \frac{dT_H}{dt} \tag{7}$$

By substituting equation (6) for T_G and rearranging,

$$\frac{dT_H}{dt} = \frac{A_H h_H}{W_H c}(0.55t - 0.7T_H) + \frac{P}{W_H c} \tag{8}$$

By using the methods of reference 9 and recognizing that equation (8) is a first-order linear differential equation of the general form

$$\frac{dT}{dt} + R(t)T = Q(t)$$

which has the general solution

$$Te^{\int R\,dt} = \int Qe^{\int R\,dt}\,dt + K$$

equation (8) integrates to

$$T_H = \frac{1.43P}{A_H h_H} + 0.794t - 1.134\frac{W_H c}{A_H h_H} + Ke^{-0.7\left(\frac{A_H h_H}{W_H c}t\right)} \tag{9}$$

The constant of integration K was evaluated at a reference (ambient) condition $t = t^*$, $T_H = T_H{}^*$ which yielded

$$T_H = \left(T_H{}^* - 0.794t^*\right)e^{-0.7\left(\frac{A_H h_H}{W_H c}\right)(t - t^*)} + 0.794t + \left(\frac{1.43P}{A_H h_H} - 1.134\frac{W_H c}{A_H h_H}\right)\left[1 - e^{-0.7\left(\frac{A_H h_H}{W_H c}\right)(t - t^*)}\right] \tag{10}$$

Equation (10) was compared to the experimental values of the heater temperatures for several levels of power. Best fit to experiment was obtained for values of the constants as follows:

$$W_H c = 0.036 \text{ J/K}$$

$$A_H h_H = 5.4 \times 10^2 \text{ W/K}$$

By knowing the driver chamber wall area (1.29 m^2) and the heater element area (0.97 m^2), an effective heater-to-gas heat-transfer coefficient h_H of 5.56×10^2 W/m^2-K can be found. Also, the gas-to-wall heat-transfer coefficient h_w is 9.77×10^2 W/m^2-K. (Eq. (6) lumps h_w and all other factors into the coefficient of t which is equal to the quantity 0.55.)

In figure 9(a), the results of a 0.325-MW application of power to the heater are compared to the results of equations (6) and (10), which are based on data of previous experiments. As seen in figure 9(a), good agreement exists between equation (10) and the experimental element temperature, whereas the theory of reference 8 underpredicted the element temperature by approximately 20 percent (see fig. 8). A comparison of equation (6) to the gas temperature T_G, calculated from pressure rise, in figure 9(a), shows that the gas temperature now can be predicted to within 10 percent of the calculated gas temperature T_G, whereas the theory of reference 8 is off by approximately 200 percent (see fig. 8).

Also presented in figure 9(a) is the diaphragm temperature and the gas temperature within the double diaphragm section. A thermocouple was attached on the downstream side of the diaphragm that sealed the driver chamber. This measured diaphragm temperature is reasonably close to the driver gas temperature, thereby indicating that there may not be as low a gas temperature at this end of the driver chamber as had been

previously thought. The temperature rise of the gas within the double diaphragm section was calculated from measured pressure rise and is presented to show that there is a gas temperature rise but that this is small compared to other parameters.

Because of the temperature variations in the heater element, the preceding results have shown driver gas temperatures below that which had been expected. Thus, to raise the driver gas temperature (as measured by the pressure rise), the obvious step would be to raise the average element temperature. Several tests were conducted in which the power was turned on to the heater and the heater element was allowed to reach maximum desired temperature; then power was turned off. When the element temperature had fallen appreciably, the power was again turned on until the maximum allowable temperature had been reached. This cycling of the electrical power was continued until very little further gas temperature rise could be obtained in a cycle. Again pressure rise indicated temperature rise.

A comparison of figure 9(a), constant power of 0.325 MW, to figure 9(b), interrupted power of 0.75 MW, shows that for about 50 seconds more time expended the interrupted power cycle will allow the average element temperature to approach its established maximum operating temperature (ΔT = 815 K - 260 K) and results in a higher gas temperature. Also, equations (6) and (10) show excellent agreement with the driver gas temperature and the driver heater element temperature. Cycling of the electrical power also allows for closer control of the element temperature.

Figure 10 is a summary of the gas temperatures for constant and interrupted power cycles. This figure emphasizes the need to operate on interrupted power cycles, for even at the same power level the average gas temperature is considerably higher when using the interrupted power cycle.

Experimental shock Mach numbers versus pressure ratio are presented in figure 11. Also presented are the theoretical Mach numbers for two different temperature ratios with helium as the driver gas and air as the driven gas. The data in all cases correspond closely to a ratio of $T_4/T_1 = 1.6$ and are in fair agreement with theory for this temperature ratio. However, for high pressure ratios, the data tend to exceed theory. References 10 and 11 have discussed this discrepancy between theory and experiment and conclude that larger than expected Mach numbers are caused by succeeding compression waves (caused by the finite opening time of the diaphragm) accelerating the shock front to its final speed.

CONCLUDING REMARKS

An experimental investigation of the heating characteristics of an internal resistance heating element was conducted in the Langley 6-inch expansion tube of the Langley

hot gas radiation research facility to obtain actual operating conditions, to compare these results to theory, and to determine whether any modification need be made to the heater element. The heater was operated in pressurized helium from 1.38 MN/m^2 to 62.1 MN/m^2. This investigation revealed large temperature variations within the heater element caused primarily by area reduction at insulator locations. These large temperature variations were reduced by welding small tabs over all grooves. This experience has shown that a constant area heater element is preferred. Previous predictions of heater element and driver gas temperatures were unacceptable so new equations were derived. These equations predict element and gas temperatures within 10 percent of the test data when either the constant power cycle or the interrupted power cycle is used. The interrupted power cycle is shown to produce a higher average element temperature and, therefore, a higher average driver gas temperature. Visual observation of the heater element, when exposed to the atmosphere and with power on, resulted in a decision to limit the heater element to 815 K. Experimental shock Mach numbers are in good agreement with theory.

Langley Research Center,
National Aeronautics and Space Administration,
Hampton, Va., October 30, 1972.

REFERENCES

1. Trimpi, Robert L.: A Preliminary Theoretical Study of the Expansion Tube, a New Device for Producing High-Enthalpy Short-Duration Hypersonic Gas Flows. NASA TR R-133, 1962.

2. Jones, Jim J.; and Moore, John A.: Exploratory Study of Performance of the Langley Pilot Model Expansion Tube With a Hydrogen Driver. NASA TN D-3421, 1966.

3. Trimpi, Robert L.; and Callis, Linwood B.: A Perfect-Gas Analysis of the Expansion Tunnel, a Modification to the Expansion Tube. NASA TR R-223, 1965.

4. Trimpi, Robert L.: A Theoretical Investigation of Simulation in Expansion Tubes and Tunnels. NASA TR R-243, 1966.

5. Sturgeon, R. F.; and Alford, D. E.: An Experimental Investigation of Internal Resistance Shock Tube Driver Gas Heating Systems. ER 7823 (Contract NAS 8-11349), Lockheed-Georgia Co., Apr. 26, 1965. (Available as NASA CR-68771.)

6. Smith, C. E.; Hajjar, D. G.; and Reinecke, W. G.: A Study of Large, High-Performance Shock Tunnel Drivers. AFAPL-TR-67-73, U.S. Air Force, July 17, 1967.

7. Baumeister, Theodore, ed.: Marks' Mechanical Engineers' Handbook. Sixth ed., McGraw-Hill Book Co., Inc., 1958.

8. Sturgeon, R. F.; Little, B. H., Jr.; and Tatom, J. W.: Shock Tube Driver Gas Heating Techniques. ER 6677 (Contract NAS 8-11078), Lockheed-Georgia Co., 1964.

9. Spiegel, Murray R.: Applied Differential Equations. Second ed., Prentice-Hall, Inc., c.1967.

10. White, Donald R.: Influence of Diaphragm Opening Time on Shock-Tube Flows. J. Fluid Mech., vol. 4, pt. 6, Nov. 1958, pp. 585-599.

11. Satofuka, Nobuyuki: A Numerical Study of Shock Formation in Cylindrical and Two-Dimensional Shock Tubes. ISAS Rep. No. 451, Univ. of Tokyo, 1970.

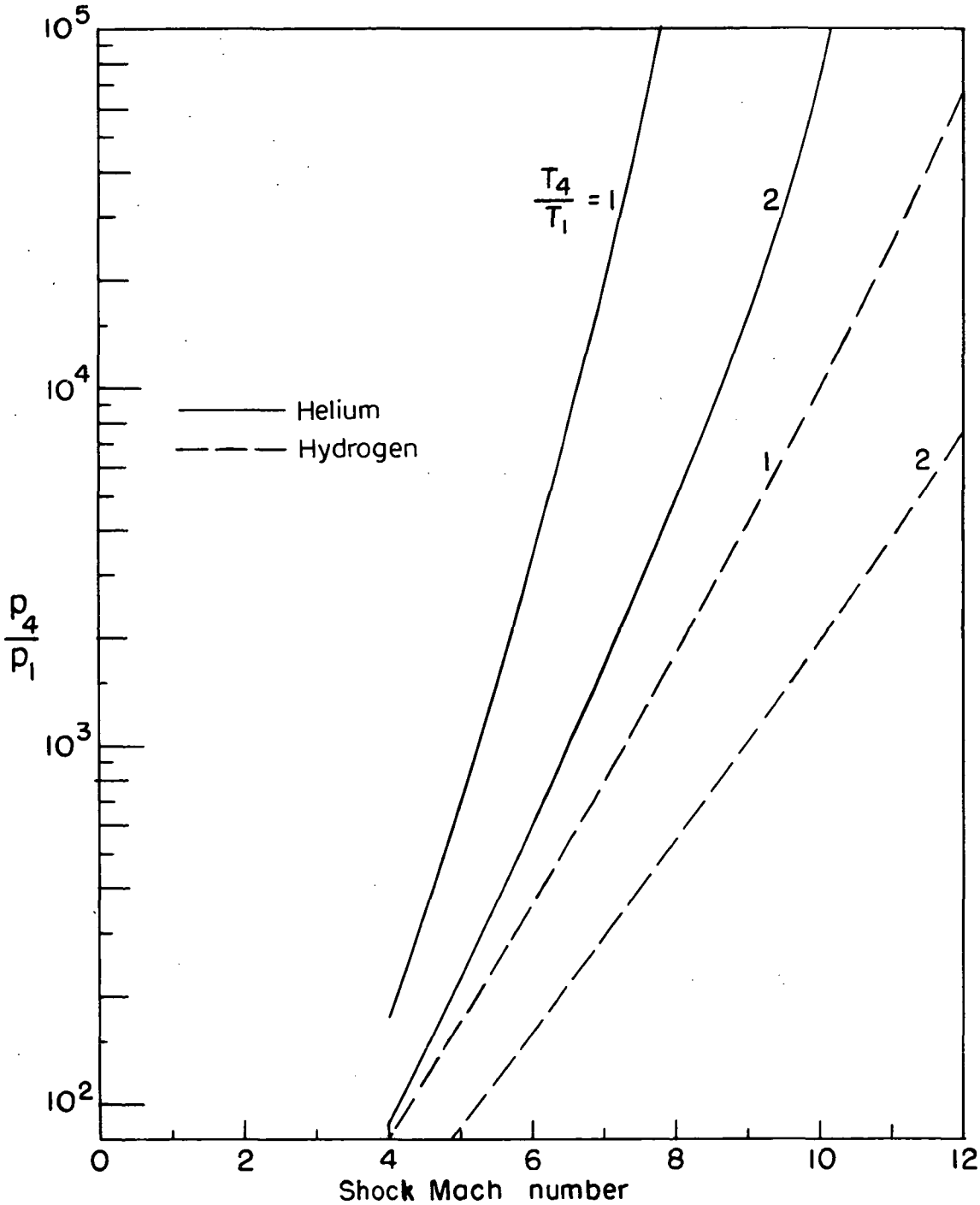

Figure 1.- Effect of driver gas temperature on shock Mach number.

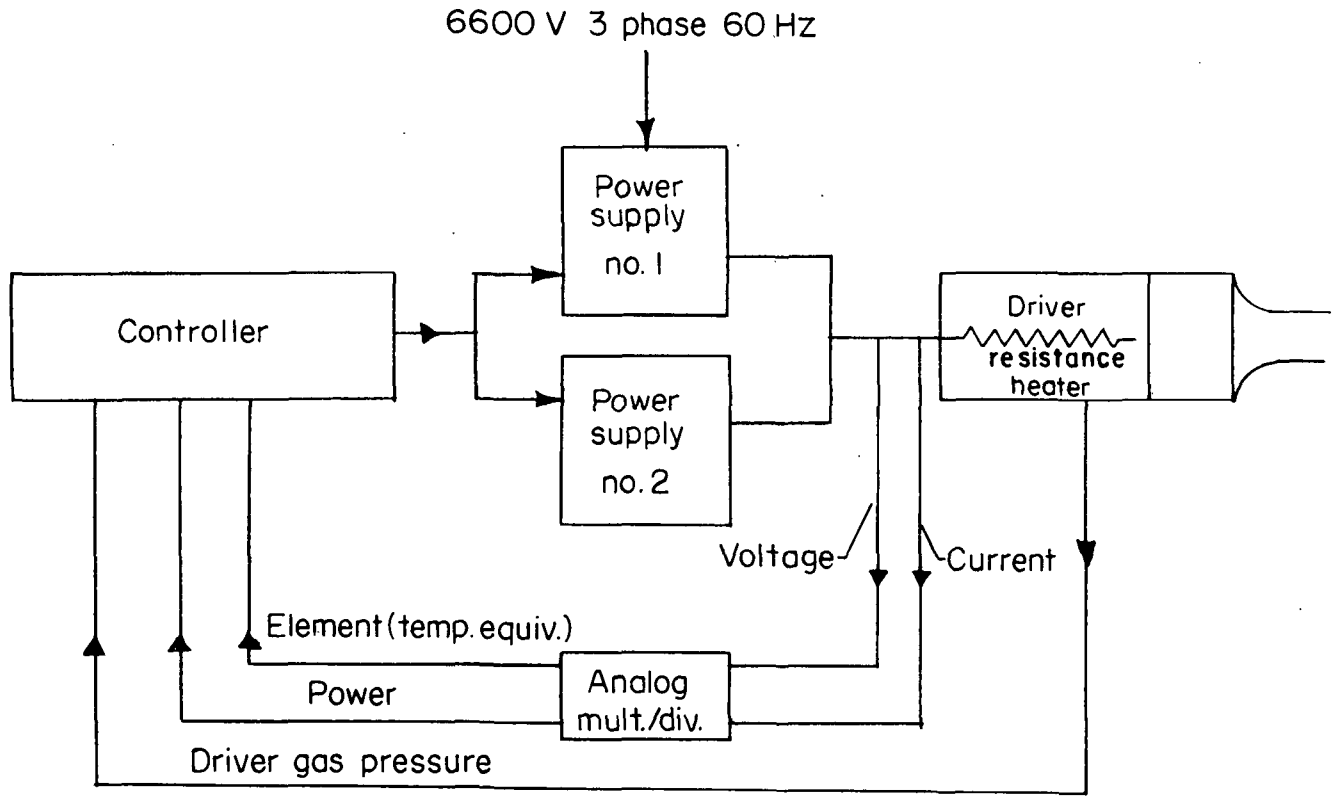

Figure 2.- Schematic diagram of electrical heating system in Langley 6-inch expansion tube.

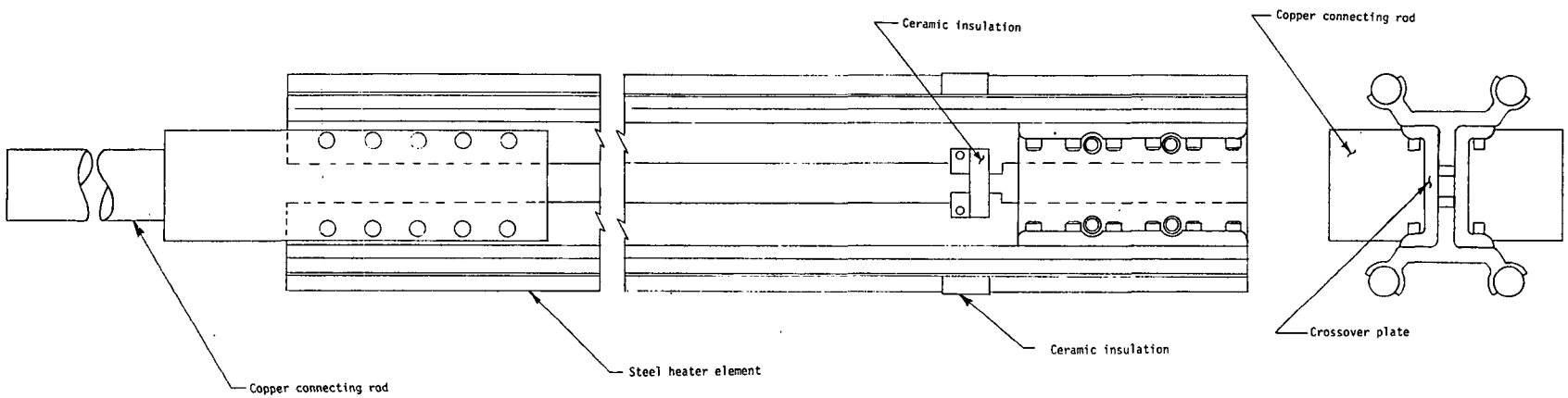

Figure 3.- Electrical resistance heating element for Langley 6-inch expansion tube driver.

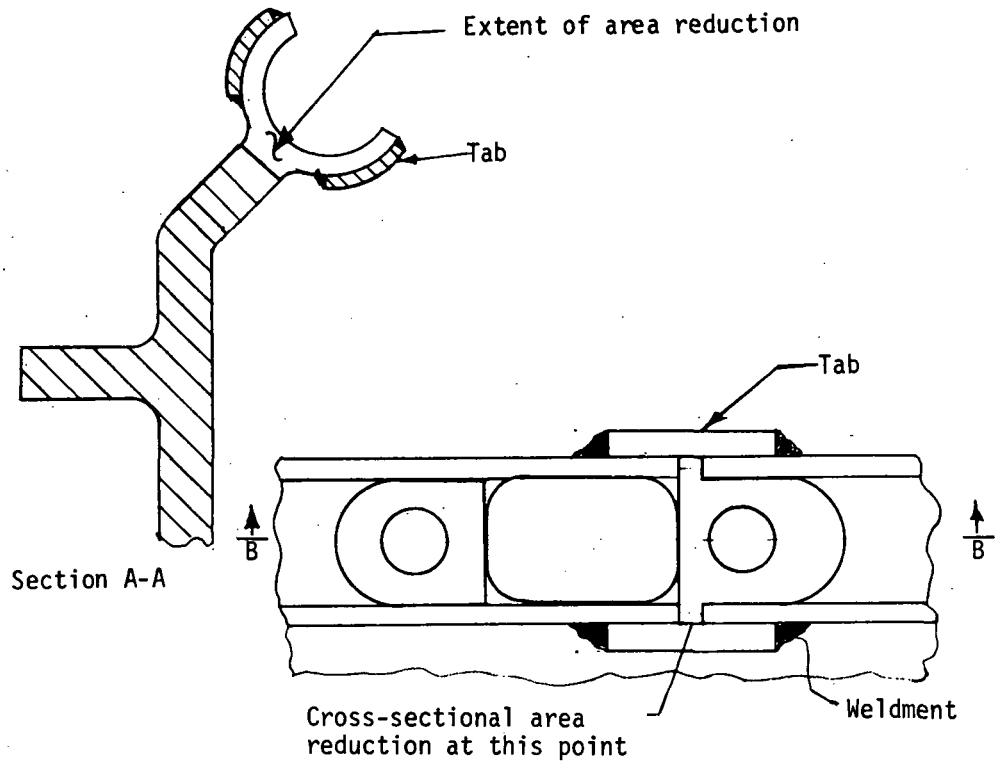

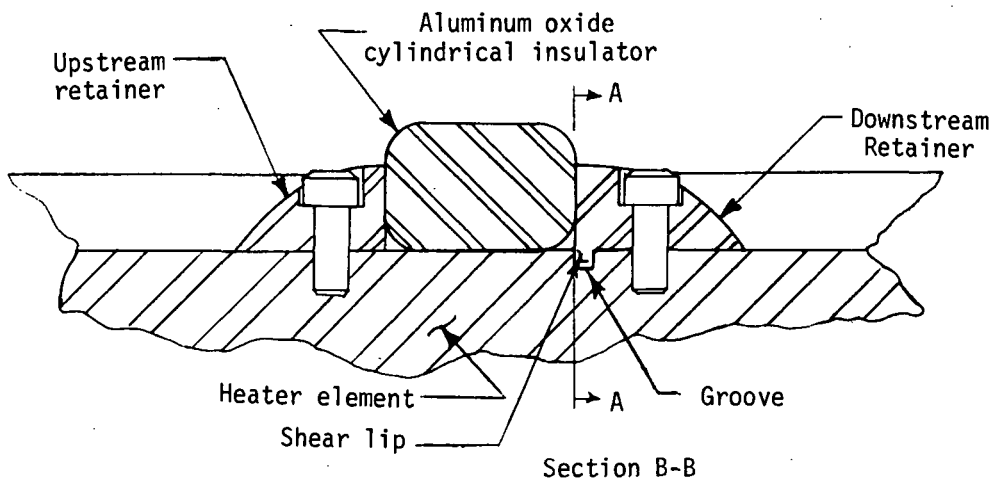

Figure 4.- Sketch of insulator and retainers causing cross-sectional area reductions with view of tab cross-sectional corrections.

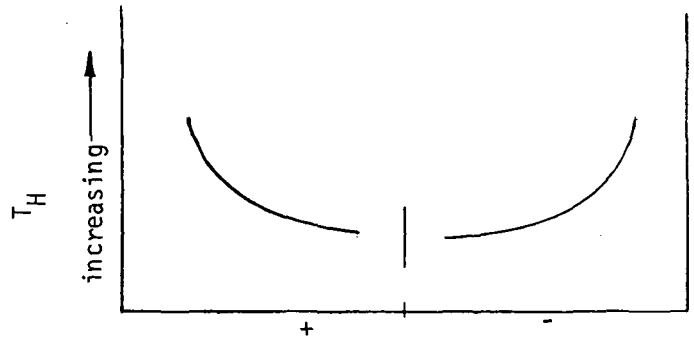

(a) Top surface.

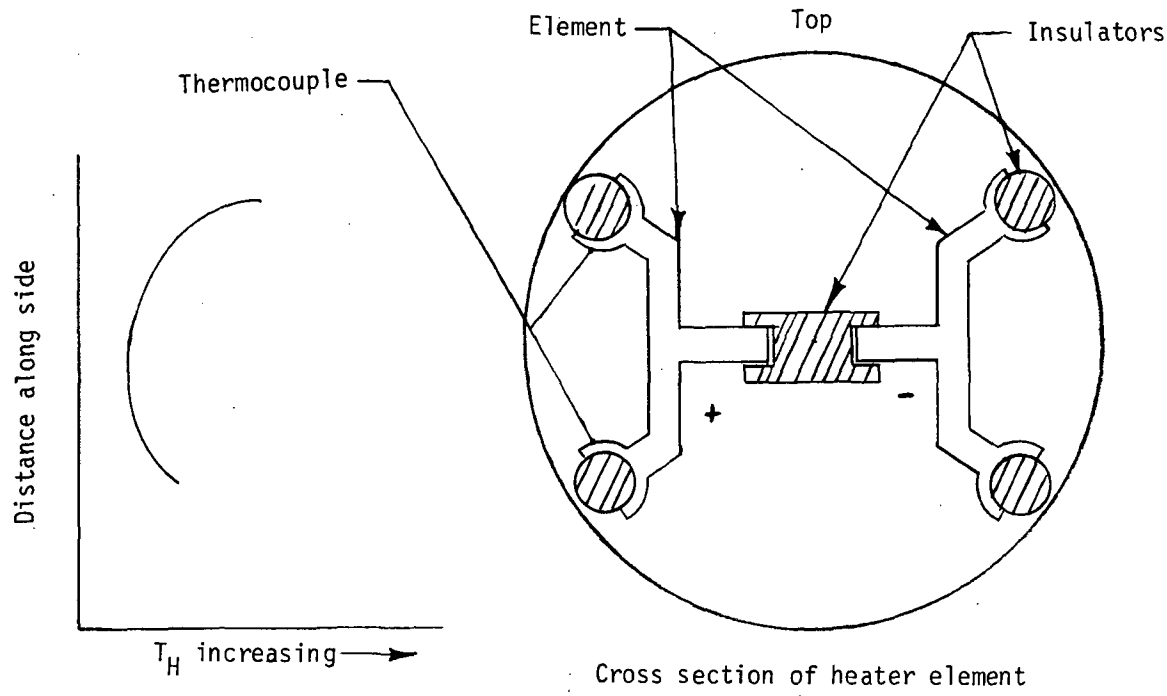

(b) Side surface.

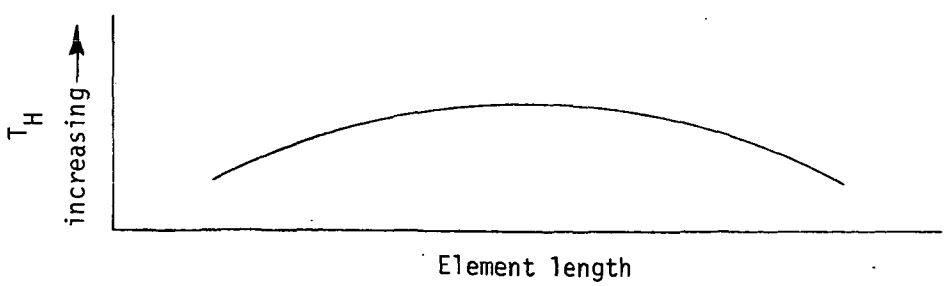

(c) Temperature along length of element.

Figure 5.- Representative heater element temperatures.

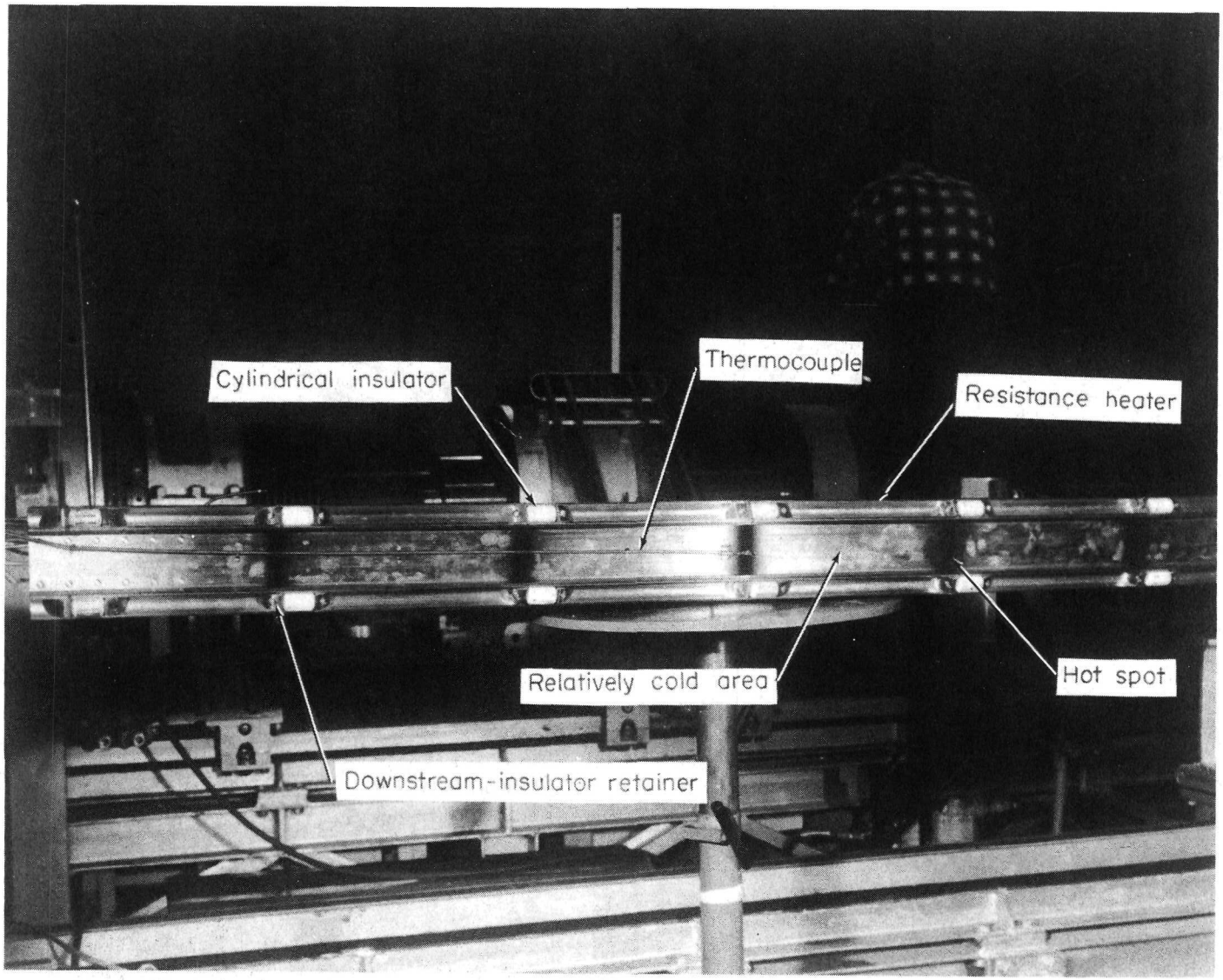

L-70-638.1

Figure 6.- Side view of internal resistance heater for Langley 6-inch expansion tube.

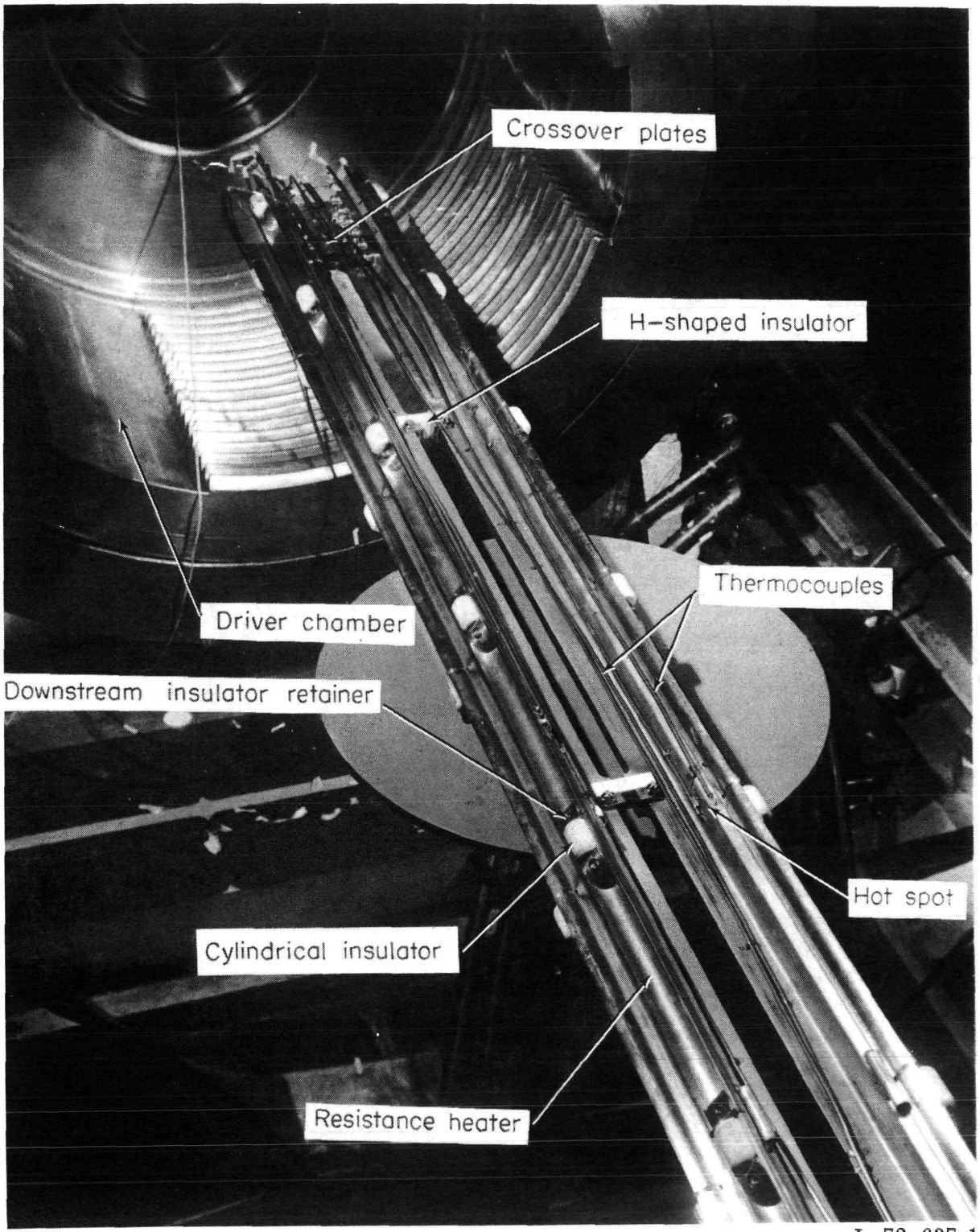

L-72-637.1

Figure 7.- Top view of internal resistance heater for Langley 6-inch expansion tube.

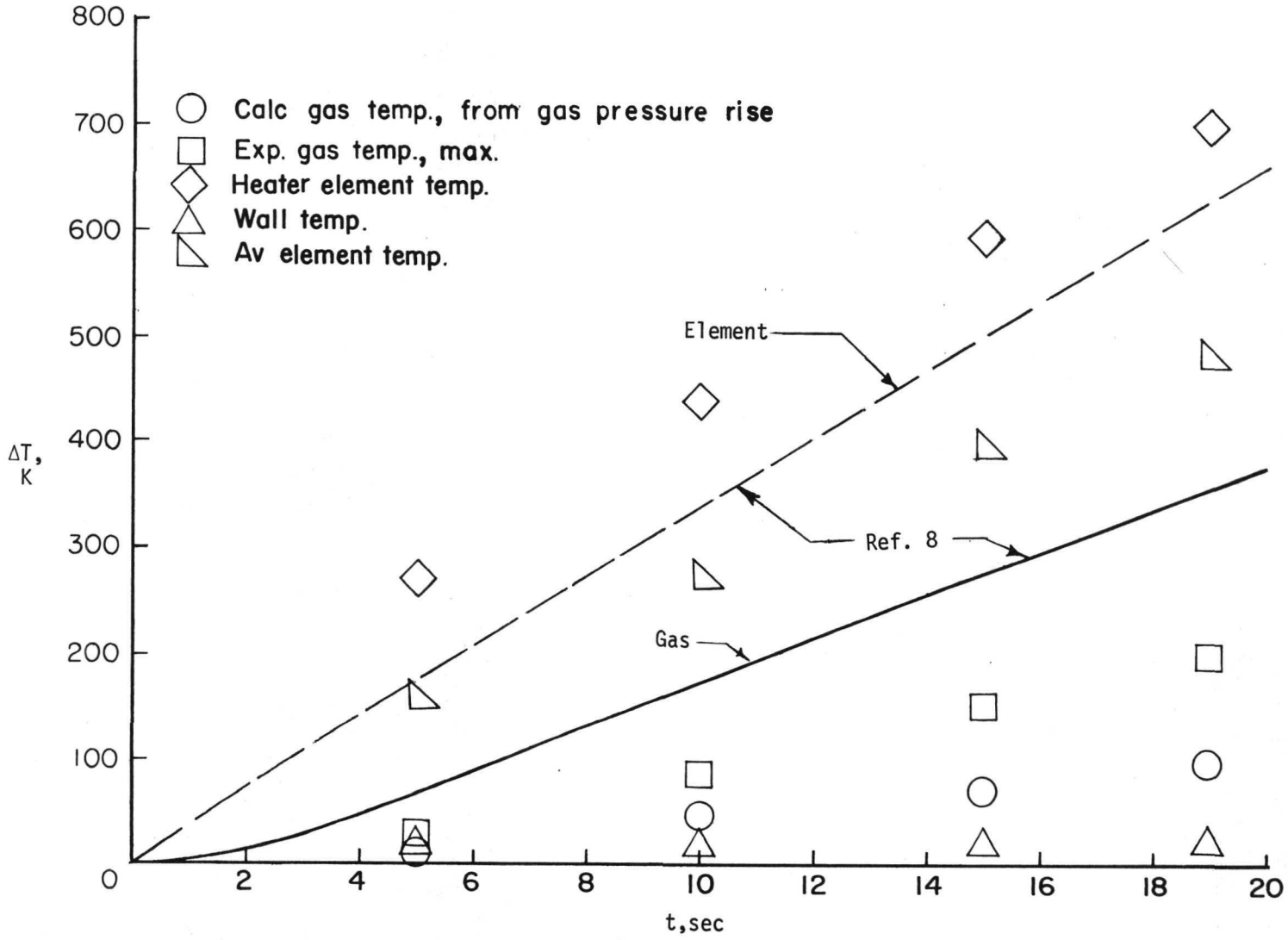

Figure 8.- Comparison of theoretical and experimental element and gas temperatures.

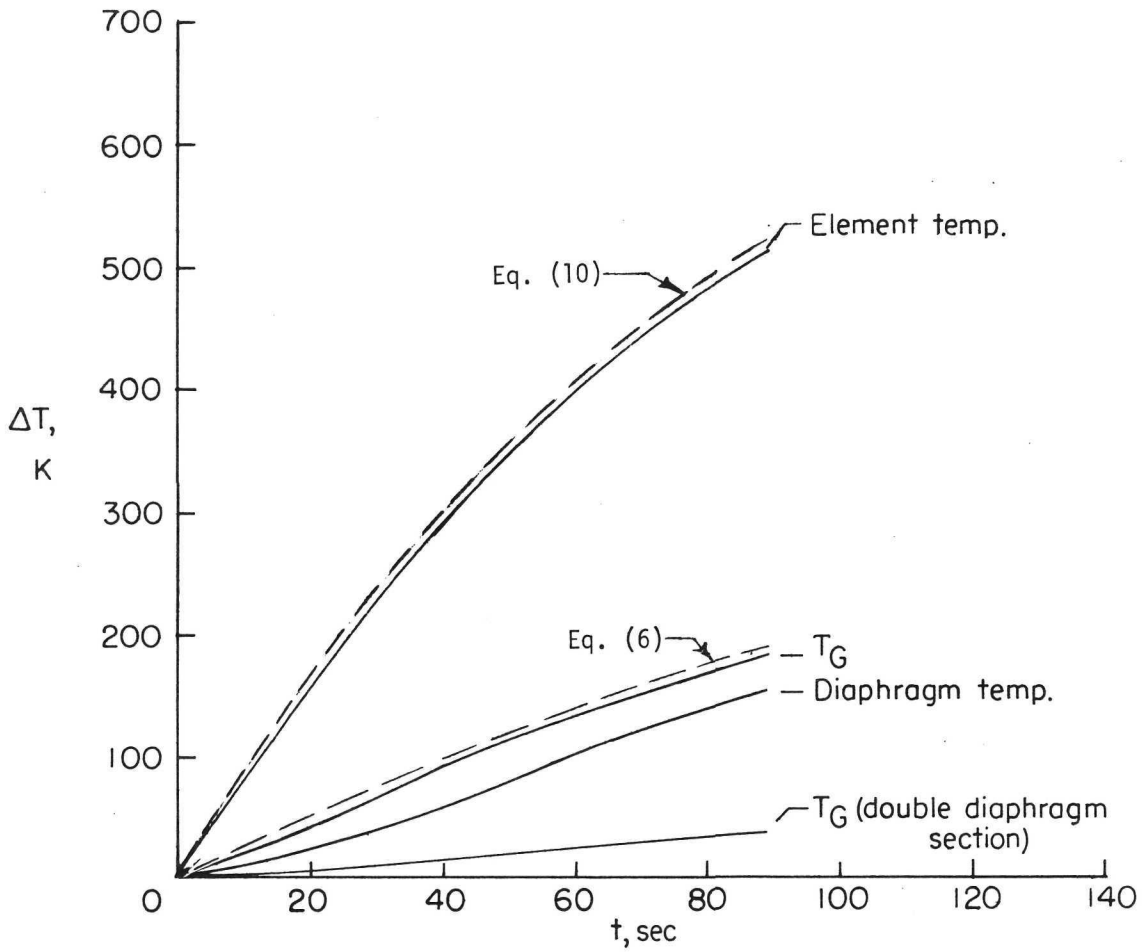

(a) Constant power cycle.

Figure 9.- Temperature histories for two power cycles.

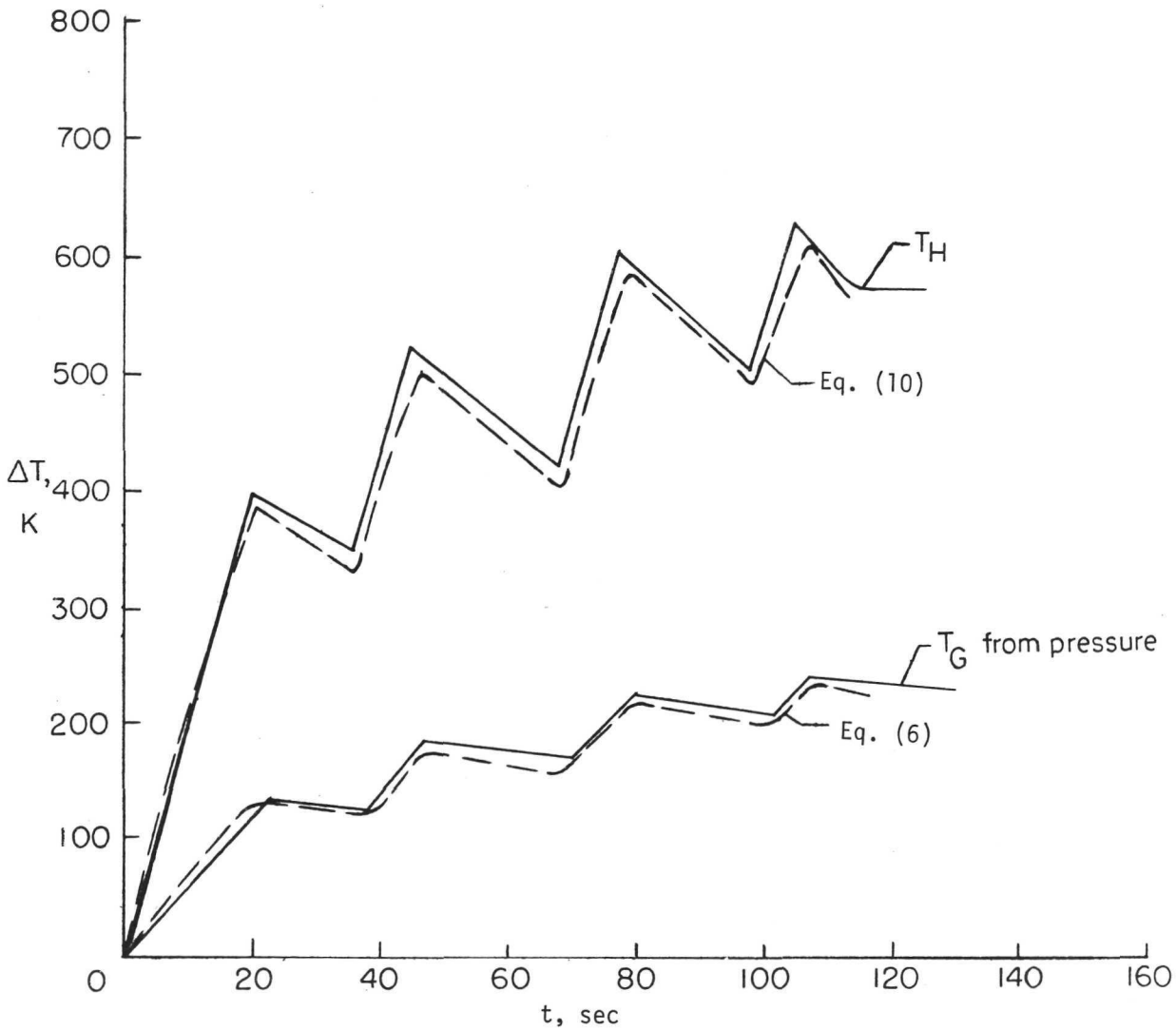

(b) Interrupted power cycle.

Figure 9.- Concluded.

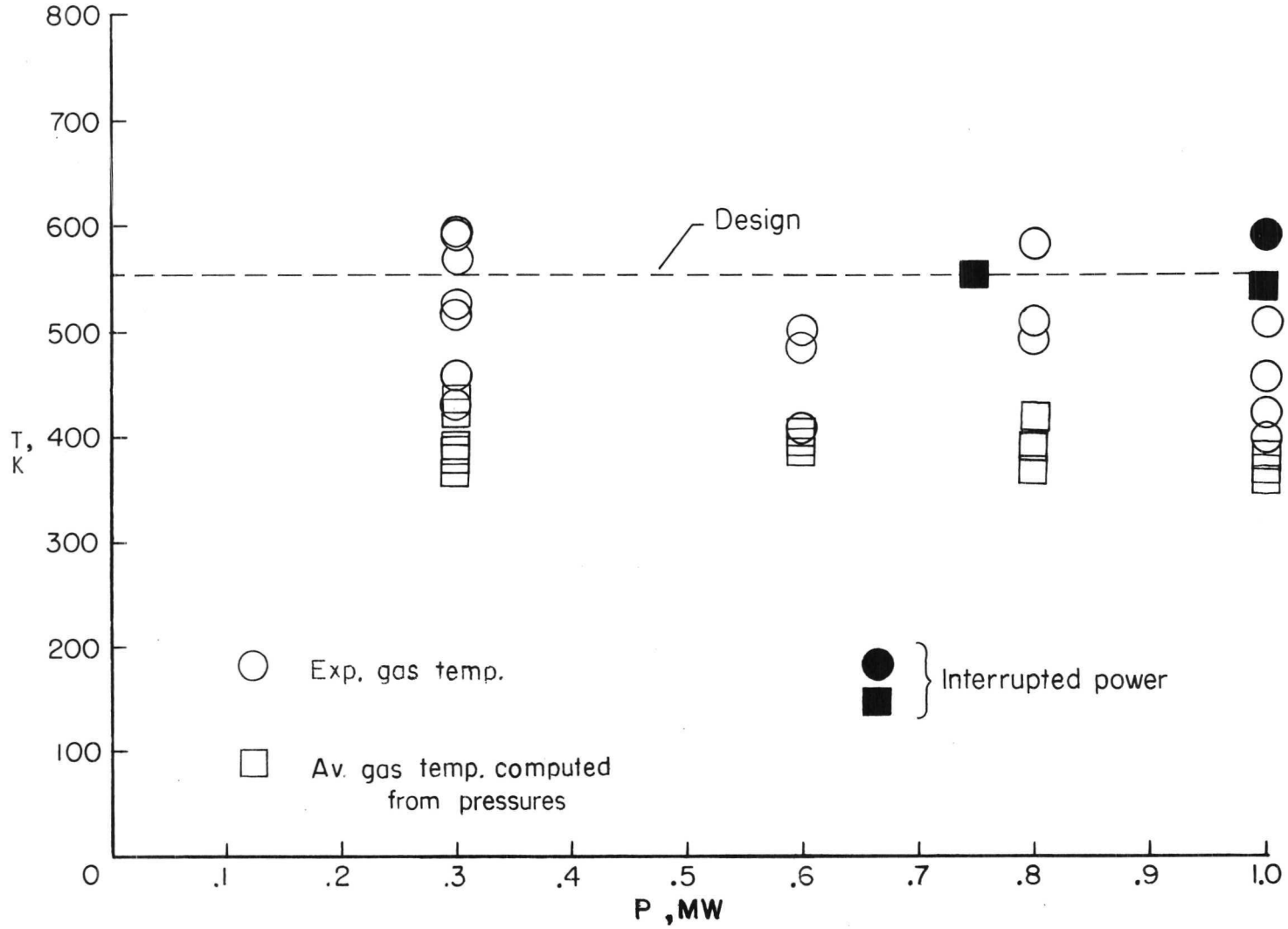

Figure 10.- Langley 6-inch expansion tube driver maximum gas temperature for various heater energy levels.

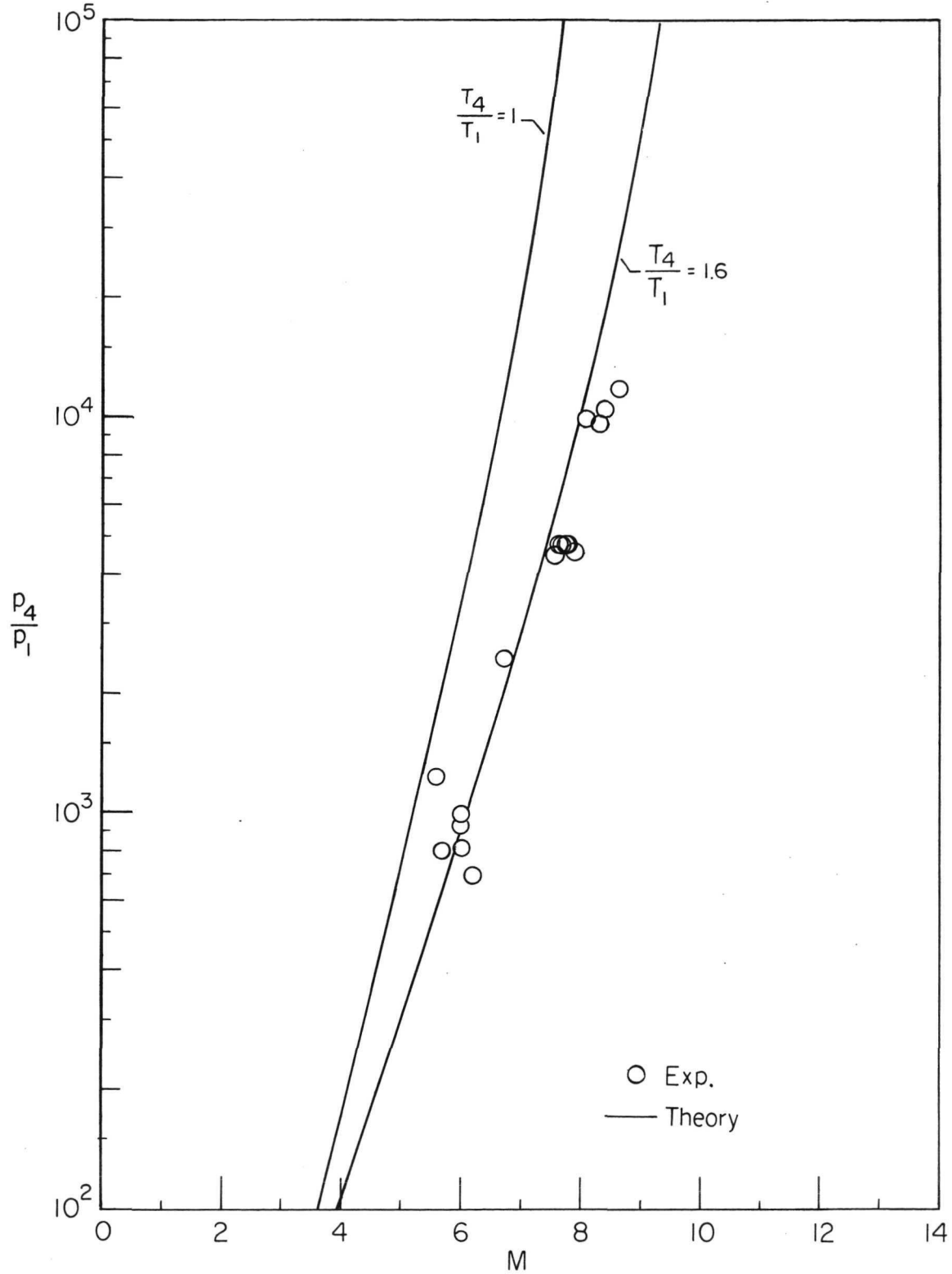

Figure 11.- Comparison of theoretical and experimental shock Mach numbers.

NATIONAL AERONAUTICS AND SPACE ADMINISTRATION
WASHINGTON, D.C. 20546

OFFICIAL BUSINESS
PENALTY FOR PRIVATE USE $300

SPECIAL FOURTH-CLASS RATE BOOK

POSTAGE AND FEES PAID
NATIONAL AERONAUTICS AND SPACE ADMINISTRATION
451

U.S.MAIL

POSTMASTER: If Undeliverable (Section 158 Postal Manual) Do Not Return

"The aeronautical and space activities of the United States shall be conducted so as to contribute . . . to the expansion of human knowledge of phenomena in the atmosphere and space. The Administration shall provide for the widest practicable and appropriate dissemination of information concerning its activities and the results thereof."

—NATIONAL AERONAUTICS AND SPACE ACT OF 1958

NASA SCIENTIFIC AND TECHNICAL PUBLICATIONS

TECHNICAL REPORTS: Scientific and technical information considered important, complete, and a lasting contribution to existing knowledge.

TECHNICAL NOTES: Information less broad in scope but nevertheless of importance as a contribution to existing knowledge.

TECHNICAL MEMORANDUMS: Information receiving limited distribution because of preliminary data, security classification, or other reasons. Also includes conference proceedings with either limited or unlimited distribution.

CONTRACTOR REPORTS: Scientific and technical information generated under a NASA contract or grant and considered an important contribution to existing knowledge.

TECHNICAL TRANSLATIONS: Information published in a foreign language considered to merit NASA distribution in English.

SPECIAL PUBLICATIONS: Information derived from or of value to NASA activities. Publications include final reports of major projects, monographs, data compilations, handbooks, sourcebooks, and special bibliographies.

TECHNOLOGY UTILIZATION PUBLICATIONS: Information on technology used by NASA that may be of particular interest in commercial and other non-aerospace applications. Publications include Tech Briefs, Technology Utilization Reports and Technology Surveys.

Details on the availability of these publications may be obtained from:

SCIENTIFIC AND TECHNICAL INFORMATION OFFICE

NATIONAL AERONAUTICS AND SPACE ADMINISTRATION

Washington, D.C. 20546